Low temperature piezoelectric and dielectric properties of lead magnesium niobate titanate single crystals

Wei Guo,[a] Dafei Jin, Wanchun Wei, and Humphrey J. Maris[a]
Department of Physics, Brown University, Providence, Rhode Island 02912, USA

Jian Tian, Xingling Huang, and Pengdi Han
H. C. Materials Corporation, 479 Quadrangle Dr., Suite E, Bolingbrook, Illinois 60440, USA

(Received 15 December 2006; accepted 26 September 2007; published online 19 October 2007)

Lead magnesium niobate-lead titanate (PMN-*x*PT) single crystal plates were prepared close to the morphotropic phase boundary with PT compositions 27%–31%. The piezoelectric and dielectric properties of these plates at liquid-helium temperature (4.2 K) were obtained by fitting measured impedance curves. In particular, the piezoelectric strain constant e_{33} is found to be in the range of 5.1–5.7 C m^{-2} at 4.2 K, which indicates an extraordinarily large piezoelectric effect compared with other materials even at such a low temperature. This result shows that PMN-*x*PT single crystals are promising candidates for ultrasonic transducers at low temperatures. © *2007 American Institute of Physics*. [DOI: 10.1063/1.2798879]

I. INTRODUCTION

Lead magnesium niobate-lead titanate [$(1-x)Pb(Mg_{1/3}Nb_{2/3})O_3$-$xPbTiO_3$, PMN-*x*PT] single crystals have excellent piezoelectric and dielectric properties at room temperature. The piezoelectric coefficient d_{33} is greater than 2000 pC/N. The electromechanical coupling factor k_{33} is greater than 90% and the maximum strain ϵ can be more than 1%.[1–3] These superior properties make PMN-*x*PT a promising candidate for the next generation ultrasonic transduction devices. The exceptional electromechanical properties of PMN-*x*PT are related to a morphotropic phase boundary (MPB) near $x=33\%-35\%$,[4] which separates the rhombohedral (pseudocubic) (3 m) and the tetragonal (4 mm) phases. The coupling between rhombohedral and tetragonal phases for crystals with near-MPB compositions enhances the dipole polarizability, allowing an optimum domain reorientation during the poling process.[1]

Up to the present time, the piezoelectric and dielectric properties for PMN-*x*PT crystals have been mostly studied at room temperature.[1,2,5,6] The investigations on PMN-*x*PT crystals at low temperatures have been primarily focused on the phase transition behavior, dielectric properties, and thermal conductivity.[7–10] The piezoelectric properties of PMN-*x*PT crystals at liquid-helium temperature (4.2 K) have not yet been systematically characterized. In this paper, we report measurements of the impedance curves for thin plates of *z*-cut PMN-*x*PT crystals containing different PT compositions ($x=27\%-31\%$) at 4.2 K. A theoretical model of the impedance of a PMN-*x*PT plate is discussed. Piezoelectric, dielectric, and elastic properties are obtained by fitting the measured impedance curves using our model.

II. THEORY

We consider a thin plate of *z*-cut PMN-*x*PT of thickness *d* sandwiched between two semi-infinite slabs of fluid (Fig. 1). The transducer is driven by an applied alternating current voltage $V(\tau)$.

For a *z*-cut plate the electric field results in a displacement in the direction of the field. In standard notation, the simplified constitutive equations of the stress field T_{II} and electric field E_{II} in region II are given by[11,12]

$$T_{\mathrm{II}} = c_{33}^{D} S_{\mathrm{II}} - h_{33} D_{\mathrm{II}}, \quad E_{\mathrm{II}} = \frac{1}{\epsilon_{33}^{S}} D_{\mathrm{II}} - h_{33} S_{\mathrm{II}}, \tag{1}$$

where S_{II} is the strain along the thickness direction and D_{II} is the electric displacement. The strain and electric field are related to the longitudinal mechanical displacement $u_{\mathrm{II}}(z,\tau)$ and the electric scalar potential $\varphi_{\mathrm{II}}(z,\tau)$ at each spatial point *z* and time τ via

$$S_{\mathrm{II}} = \frac{\partial u_{\mathrm{II}}(z,\tau)}{\partial z}, \quad E_{\mathrm{II}} = -\frac{\partial \varphi_{\mathrm{II}}(z,\tau)}{\partial z}. \tag{2}$$

Here c_{33}^{D} is the elastic stiffness constant at constant electric displacement, h_{33} is the piezoelectric pressure constant, and ϵ_{33}^{S} is the dielectric constant at constant strain.

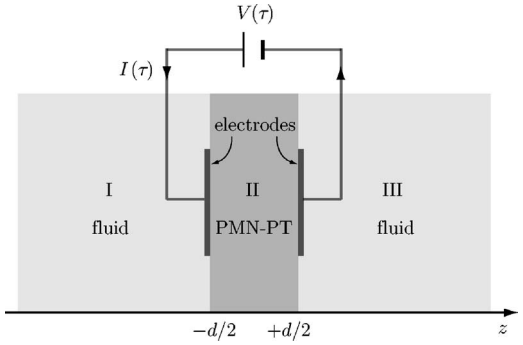

FIG. 1. A PMN-*x*PT crystal plate between two semi-infinite fluid slabs.

[a]Electronic mail: humphrey_maris@brown.edu

TABLE I. Material constants for PMN-xPT crystals at room temperature (RT) and 4.2 K.

x (%)	ρ (g cm^{-3})	d (mm)	T (K)	$\epsilon_{33}^T/\epsilon_0$	$\epsilon_{33}^S/\epsilon_0$	c_{33}^E (10^{10} N m^{-2})	v (m s^{-1})	k_t	h_{33} (10^8 V m^{-1})	e_{33} (C m^{-2})
27	8.2	0.693	RT	4370[a]	834[a] (837[b])	11.8	4540	0.55	26.4	19.5
			4.2	433[a]	(78[b])	14.7	4850	0.49	82.4	5.69
28	8.2	0.694	RT	4510[a]	814[a] (817[b])	11.6	4530	0.56	27.3	19.7
			4.2	381[a]	(72[b])	14.6	4800	0.47	80.8	5.15
29	8.2	0.705	RT	5120[a]	780[a] (786[b])	11.5	4540	0.56	27.9	19.3
			4.2	403[a]	(74[b])	14.4	4870	0.51	87.8	5.75
31	8.2	0.707	RT	6070[a]	752[a] (758[b])	11.5	4540	0.56	27.7	18.5
			4.2	420[a]	(71[b])	14.4	4860	0.49	84.3	5.30

[a]Directly measured.
[b]Obtained via fitting.

By solving the differential equations with boundary conditions for $u(z,\tau)$ and $\varphi(z,\tau)$,[11] one can obtain the surface displacements of the PMN-xPT crystal thin plate in the Fourier representation

$$u_{\mathrm{II}}\left(\pm\frac{d}{2},\omega\right)=\frac{\pm e_{33}V(\omega)}{2h_{33}^2\epsilon_{33}^S+iBq'd-c_{33}^Dqd\cot\left(\frac{qd}{2}\right)}, \tag{3}$$

where B is the bulk modulus of the loading fluid and e_{33} is the piezoelectric strain constant of PMN-xPT given by[11]

$$e_{33}=h_{33}\epsilon_{33}^S. \tag{4}$$

The wave numbers in the loading fluid and in the PMN-xPT are

$$q'=\frac{\omega}{\sqrt{B/\rho'}}=\frac{\omega}{v'},\quad q=\frac{\omega}{\sqrt{c_{33}^D/\rho}}=\frac{\omega}{v}, \tag{5}$$

where ρ' and ρ are the densities of the loading fluid and the PMN-xPT, respectively, and v' and v are the sound velocities.

The impedance of this structure is given by

$$Z(\omega)=\frac{d}{-i\omega A\epsilon_{33}^S}\left[1+\frac{2c_{33}^Dk_t^2/(Bq')}{i-\frac{c_{33}^Dq}{Bq'}\cot\left(\frac{qd}{2}\right)}\right], \tag{6}$$

where A is the electrode area and we have introduced the thickness-mode coupling coefficient k_t defined as[11]

$$k_t=h_{33}\sqrt{\frac{\epsilon_{33}^S}{c_{33}^D}}. \tag{7}$$

To be more realistic, we should also take into account the internal mechanical damping of the PMN-xPT.[12] This change adds a small imaginary part $\tilde{q}$ to the wave number q of the PMN-xPT, which is responsible for the observed broadening of the resonance peaks.

III. EXPERIMENT AND DISCUSSION

Specimens of PMN-xPT crystals with x=0.27, 0.28, 0.29, and 0.31 were prepared from a ⟨001⟩-seeded crystal grown using a modified Bridgman technique. The PT composition of each specimen was estimated from the Curie temperature (T_C) measurements. All of the crystal specimens were oriented and cut along the ⟨001⟩ crystallographic direction with dimensions of approximately $7\times7\times0.7$ mm^3. The specimens were annealed at 600 °C for 8 h. Gold electrodes were deposited onto the surfaces by sputtering.

We measured the dielectric constants at constant stress ϵ_{33}^T at room temperature in air and in liquid helium around 4.2 K using an LCR meter (Agilent 4263B) at 1 kHz and 1 V voltage level. ϵ_{33}^T was calculated by the formula

$$\epsilon_{33}^T=\frac{C}{\epsilon_0}\frac{d}{A}, \tag{8}$$

where C is the measured capacitance. At room temperature, the dielectric constant at constant strain ϵ_{33}^S was also determined from capacitance measurement at frequencies well above any of the strong resonances. The measured results of ϵ_{33}^T and ϵ_{33}^S are listed in Table I.

A radio frequency network analyzer (Agilent 8712ES) was employed for the resonance measurements of the thickness modes of our specimens. Two frequency ranges, 2–4 MHz covering the first thickness mode resonance frequency and 9–11 MHz covering the third thickness mode resonance frequency, were chosen for measuring the impedance curves of our specimens at room temperature and 4.2 K.

The fitting of the impedance curves is carried out in the following steps. First, the thickness mode coupling coefficient k_t and the elastic constant c_{33}^E are calculated from the resonance and antiresonance frequencies on the measured impedance curves by using the formulas[11]

$$k_t^2=\frac{\pi}{2}\frac{f_s}{f_p}\tan\left[\frac{\pi}{2}\frac{f_p-f_s}{f_p}\right], \tag{9}$$

$$c_{33}^E=4(1-k_t^2)\rho f_p^2d^2, \tag{10}$$

where f_s is the resonance frequency (impedance magnitude minimum) and f_p is the antiresonance frequency (impedance magnitude maximum). Here we used the room-temperature specimen density in the calculation and curve fitting at liquid-helium temperature.

Then in Eq. (6), using the known properties of the loading fluid, we adjust ϵ_{33}^S, the sound velocity v, and the damping part $\tilde{q}$ of the wave number q to get the best fit to the experimentally measured impedance curves. In this way, we can determine ϵ_{33}^S and the sound velocity v.

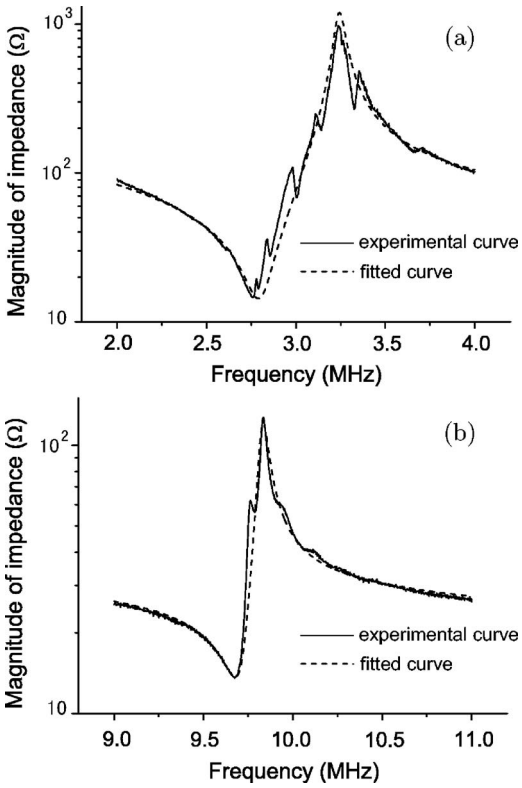

FIG. 2. Magnitude of the impedance of a PMN-0.28PT plate at room temperature. Parts (a) and (b) show the first and third resonance peaks, respectively. The solid curve shows the experimental data and the dashed curve is the fit.

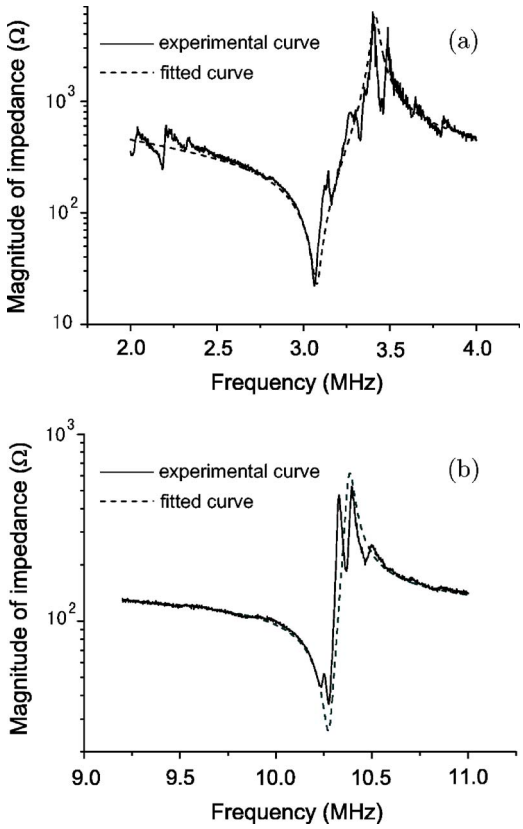

FIG. 3. Magnitude of the impedance of a PMN-0.28PT plate at 4.2 K. Parts (a) and (b) show the first and third resonance peaks, respectively. The solid curve shows the experimental data and the dashed curve is the fit.

As an example, Fig. 2 shows a fit to data obtained from a PMN-xPT specimen with $x=0.28$ at room temperature. The small peaks on the measured curves are due to a weak coupling to modes other than the thickness mode of the specimen and their amplitudes are influenced by the way that electrical contact is made to the specimen and the exact placement of the specimen in the holder. The fitted results for this specimen show good agreement with the directly measured values (Table I), indicating that our fitting method works well.

The obtained values of dielectric constants ϵ_{33}^{T}, ϵ_{33}^{S}, elastic constants c_{33}^{E}, piezoelectric pressure constants h_{33}, piezoelectric strain constants e_{33}, sound wave velocity v, and thickness coupling coefficient k_t for all our PMN-xPT crystal $(x=0.27,0.28,0.29,0.31)$ at room temperature and 4.2 K are given in Table I. For comparison, the directly measured ϵ_{33}^{S} at room temperature are also shown in the table. A typical fitting of the measured impedance curve at 4.2 K is shown in Fig. 3.

Our results (Table I) show that the thickness coupling coefficient k_t for different PT compositions depends weakly on temperature. The dielectric constants with constant strain or constant tension both decrease significantly with temperature for all specimens. The elastic constants c_{33}^{E} and sound wave velocities v of the specimens increase with decreasing temperature.

According to Eq. (3), if the internal damping of the transducer is ignored, it is easy to show that if we drive the transducer in liquid helium at the resonance frequency for a long enough time, the final surface displacement the transducer can achieve is approximately given by

$$u_{\mathrm{II}}\left(\pm\frac{d}{2},\omega_r\right)\simeq\frac{\pm e_{33}V(\omega_r)}{i\rho' v'\omega_r d}, \tag{11}$$

where $V(\omega_r)$ is the voltage on the transducer at resonance frequency ω_r. We see that e_{33} is the only material constant that appears in the earlier formulas and thus a large e_{33} constant is required in order to have a large magnitude of the surface displacement at a fixed external voltage. Although the finite internal damping of the material may change the earlier result to some extent, the e_{33} constant is still the dominant factor in determining the magnitude of surface displacement.

In Table II, we list the relevant material constants for z-cut lithium niobate and lithium tantalate together with our PMN-0.29PT. Due to its larger e_{33}, PMN-xPT is indeed a

TABLE II. Measured dielectric, piezoelectric, and thickness coupling constants of PMN-0.29PT in thickness mode compared with other materials.

Material	T (K)	$\epsilon_{33}^{S}/\epsilon_0$	e_{33} (C m^{-2})	k_t
PMN-0.29PT	RT	780	19.3	0.56
	4.2	74	5.75	0.51
$LiNbO_3$ [a]	RT	27.9	1.33	0.17
$LiTaO_3$ [a]	RT	42.8	1.09	0.19

[a]All data from Ref. 13.

very promising choice for physics experiment at low temperatures. We list room temperature values for lithium niobate and tantalate because we have been unable to find in the literature low temperature values of e_{33} for these materials and because, at least in the temperature range around room temperature, their piezoelectric constants depend weakly on temperature.[13]

IV. CONCLUSION

Based on the results of our measurements and fittings, we can see that PMN-*x*PT crystals retain a strong piezoelectric effect at liquid-helium temperature. These materials should be particularly useful for studies of liquid helium itself. The acoustic impedance of liquid helium is very small compared to that of conventional solid materials and consequently to generate a sound wave of high intensity in liquid helium it is necessary to use a transducer that can provide a large surface displacement.

ACKNOWLEDGMENTS

This work was supported in part by the National Science Foundation through Grant No. DMR-0605355 and by the Office of Naval Research under Grant No. N00014-03-M-0219. The authors would like to thank William Patterson for his assistance with the experiment and Mingsen Guo for helpful discussions.

[1] S.-E. Park and T. R. Shrout, IEEE Trans. Ultrason. Ferroelectr. Freq. Control **44**, 1140 (1997).
[2] R. Zhang, B. Jiang, and W. Cao, J. Appl. Phys. **90**, 3471 (2001).
[3] R. F. Service, Science **275**, 1878 (1997).
[4] S. W. Choi, J. M. Jung, and A. S. Bhalla, Ferroelectr., Lett. Sect. **21**, 27 (1996).
[5] H. Cao and H. S. Luo, Ferroelectrics **274**, 309 (2002).
[6] Y. P. Guo, H. S. Luo, K. P. Chen, H. Q. Xu, X. W. Zhang, and Z. W. Yin, J. Appl. Phys. **92**, 6134 (2002).
[7] F. M. Bai, N. G. Wang, J. F. Li, D. Viehland, P. M. Gehring, G. Y. Xu, and G. Shirane, J. Appl. Phys. **96**, 1620 (2004).
[8] S. Priya, D. Viehland, and K. Uchino, Appl. Phys. Lett. **80**, 4217 (2002).
[9] D. M. Zhu and P. D. Han, Appl. Phys. Lett. **75**, 3868 (1999).
[10] X. M. Wan, R. K. Zheng, H. L. W. Chan, C. L. Choy, X. Y. Zhao, and H. S. Luo, J. Appl. Phys. **96**, 6574 (2004).
[11] ANSI/IEEE Std. 176-1987, *IEEE Standard on Piezoelectricity* (IEEE, New York, 1987).
[12] *Physical Acoustics: Principles and Methods*, edited by W. P. Mason (Academic, New York, 1964).
[13] R. T. Smith and F. S. Welsh, J. Appl. Phys. **42**, 2219 (1971).